

Effective coordination number: A simple indicator of activation energies for NO dissociation on Rh(100) surfaces

Prasenjit Ghosh,^{1,2} Raghani Pushpa,³ Stefano de Gironcoli,³ and Shobhana Narasimhan²

¹*The Abdus Salam International Centre for Theoretical Physics (ICTP), Strada Costiera 11, I-34151 Trieste, Italy*

²*Jawaharlal Nehru Centre for Advanced Scientific Research, Jakkur PO, Bangalore 560 064, India*

³*Scuola Internazionale Superiore di Study Avanzati (SISSA), Via Beirut 2/4, I-34151 Trieste, Italy*

(Received 17 August 2009; published 15 December 2009)

We have used density-functional theory to compute the activation energy for the dissociation of NO on two physical and two hypothetical systems: unstrained and strained Rh(100) surfaces and monolayers of Rh atoms on strained and unstrained MgO(100) surfaces. We find that the activation energy, relative to the gas phase, is reduced when a monolayer of Rh is placed on MgO, due both to the chemical nature of the substrate and the strain imposed by the substrate. The former effect is the dominant one, though both effects are of the same order of magnitude. We find that both effects are encapsulated in a simple quantity which we term as the “effective coordination number” (n_e); the activation energy is found to vary linearly with n_e . We have compared the performance of n_e as a predictor of activation energy of NO dissociation on the above-mentioned Rh surfaces with the two well-established indicators, namely, the position of the d -band center and the coadsorption energy of N and O. We find that for the present systems n_e performs as well as the other two indicators.

DOI: [10.1103/PhysRevB.80.233406](https://doi.org/10.1103/PhysRevB.80.233406)

PACS number(s): 28.52.Fa, 68.43.Bc, 96.12.Kz, 71.20.Be

Catalysts are vital to the present-day chemical industry and are also important in the search for alternative and cleaner energy sources. However, most catalysts that are in use today have been developed by a process of trial and error, and replacing this by a program of rational design is one of the grand challenges in chemistry today. Theoretical calculations using density-functional theory (DFT) can help provide insight and guiding principles since they can supply detailed microscopic information about the various elementary steps in a reaction.¹ They also allow one to explore hypothetical systems that, even if impossible to create in the laboratory, can help one to discern patterns that can then provide guidelines for the design process.

In this Brief Report, we focus on one particular reaction: the dissociation of NO, which is one of the steps in converting undesirable NO_x gases to N₂, for example, in catalytic converters in automobiles; Rh has been shown to be one of the best catalysts for this process.^{2–4} In catalytic converters, small particles of the metal catalyst are placed on a ceramic substrate. This situation is quite different from the ideal and clean single-crystal metal surfaces that have traditionally been studied using the techniques of surface science. In recent years, however, there has been increasing attention paid to more realistic situations, such as the presence of asperities and defects, finite particle sizes, and the influence of the substrate. The substrate can affect the operation of a catalyst in various ways since it changes the environment of the metal catalyst atoms: they can have different neighbors, and may also be strained due to the presence of the substrate. Here we consider four model systems that enable us to explore the effects of changing the local environment of catalyst atoms: (a) a Rh(100) surface, (b) a Rh(100) surface where both the surface and substrate have been stretched (by 9.9%) to the larger lattice constant of MgO, (c) a monolayer of Rh/MgO(100), where the MgO substrate has been compressed to have the same lattice constant as that of bulk Rh, and (d) a pseudomorphic monolayer of Rh/MgO(100). These are the same systems for which we had earlier computed

adsorption energies.⁵ We note that systems (a) and (b) are related by strain, as are systems (c) and (d), while systems (a) and (c), and systems (b) and (d), differ only in the chemical nature of the substrate. Only system (a) may be “real”—systems (b) and (c) are hypothetical while it is not known whether system (d) corresponds to a realistic experimental structure.

We have performed spin-polarized DFT calculations using the PWSCF package of the QUANTUM-ESPRESSO distribution,⁶ ultrasoft pseudopotentials,⁷ and a plane-wave basis with a cutoff of 30 Ry. Exchange and correlation effects are treated using the generalized gradient approximation, in the Perdew-Burke-Ernzerhof form.⁸ In order to improve convergence a Methfessel-Paxton smearing⁹ with a width of 0.03 Ry was used. The calculations have been performed with a (2×3) surface unit cell and a vacuum of about 14 Å. For (a) and (b), the systems have been modeled using a four-layer Rh slab, of which only the top two layers are relaxed. For (c) and (d), the MgO substrate has been modeled by a four-layer MgO slab with a monolayer of Rh on top of it; the Rh monolayer and the top two MgO layers are permitted to relax. Brillouin-zone integrations have been performed using a $(6 \times 4 \times 1)$ Monkhorst-Pack¹⁰ k -point mesh. We note that all the above calculational details are identical to those used in our earlier work on adsorption.⁵

In order to test the performance of the pseudopotentials used by us, we first calculated the bulk lattice parameters of Rh and MgO and the N-O bond length in gas phase and compare the results with experimental measurements and previous calculations. We obtained a value of 3.85 Å for the lattice constant of bulk Rh, which is in excellent agreement with the experimental value of 3.80 Å,¹¹ and previous theoretical values of 3.87 Å.¹² For MgO, we obtained a lattice constant of 4.25 Å, which is identical to the value obtained in previous calculations,¹³ and in good agreement with the experimental value of 4.21 Å.¹⁴ For NO in the gas phase, we obtained a binding energy of 7.13 eV, and an N-O bond length of 1.17 Å. For comparison, the experimental values are 6.5 eV and 1.15 Å, respectively.¹⁵

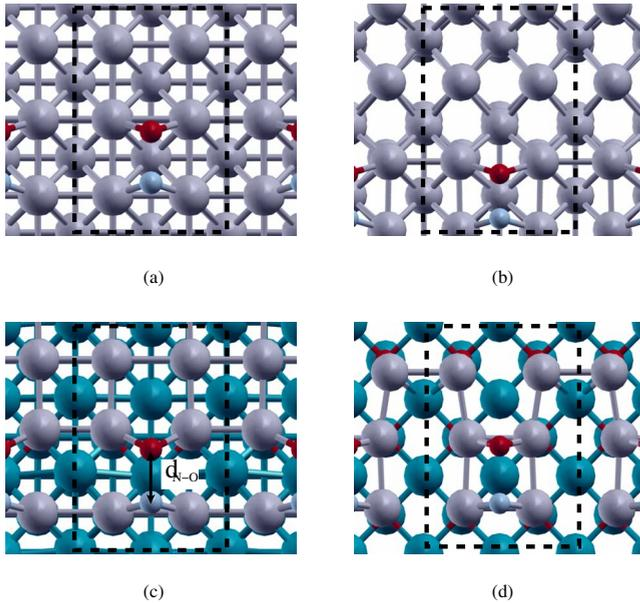


FIG. 1. (Color online) The transition states of NO dissociation for cases (a), (b), (c), and (d). Light blue (small gray), red (black), gray and dark blue (dark gray) spheres represent N, O, Rh, and Mg atoms, respectively. The dashed black line denotes the surface unit cell considered in our calculations.

The reaction paths, transition states and the barriers for NO dissociation have been calculated using the climbing-image nudged elastic band method.¹⁶ The initial state consists of NO adsorbed on the surface: for cases (a) and (b), the NO molecule sits vertically on the surface, with the N bonded to two Rh atoms and sitting above a bridge site. For these two cases, the NO binding energies (with respect to NO molecules in gas phase) are -2.59 and -2.86 eV, respectively. However, in cases (c) and (d), the stable adsorption geometry consists of NO lying down on the surface, slightly tilted, with both N and O atoms bonded to Rh atoms, the NO binding energies (with respect to NO molecules in gas phase) being -3.38 eV and -4.08 eV, respectively. For cases (a) and (b), as the reaction progresses, the NO molecule first rotates away from the vertical to a near-horizontal position. In all four cases, the N-O bond then stretches until it breaks. The transition states for all the four cases are shown in Fig. 1. In the “final” state corresponding to the reaction intermediates, N and O are coadsorbed on the surface, occupying either nearest-neighbor or next-nearest-neighbor hollow sites (Fig. 2). As an example we show the reaction path for case (a) in Fig. 3.

Upon computing the activation energy, E_a , relative to the gas phase NO, using the expression $E_a = E_{TS} - E_{slab} - E_{NO}$, where E_{TS} is the total energy of the transition state (TS), E_{slab} is the total energy of the clean slab and E_{NO} is the energy of the NO molecule in the gas phase, we obtain values of -1.96 , -2.38 , -2.90 , and -3.61 eV for cases (a), (b), (c), and (d), respectively. We also compute the coadsorption energy E_{coads} , using the formula $E_{coads} = E_{N+O:slab} - E_{slab} - E_{NO}^{gas}$, where $E_{N+O:slab}$ is the total energy of the slab with the NO molecule dissociated on it. We find that like E_a , E_{coads} is also progressively lowered from -3.34 to -3.47 to -4.88 to

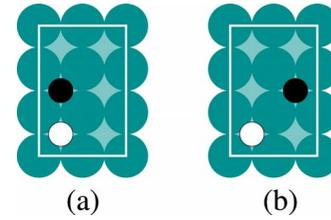


FIG. 2. (Color online) Top view of the geometries considered for N and O coadsorption on Rh(100) surfaces. The cyan, white, and black circles represent Rh, O, and N atoms, respectively. In configuration (a), N and O are at nearest-neighbor hollow sites, in (b) N and O are at diagonally opposite hollow sites.

-5.04 eV [for all the cases, the N and O coadsorption geometries correspond to that of Fig. 2(b)]. A lower barrier is obviously favorable from the point of view of dissociation of the N-O bond; however, too low a value of E_{coads} may hinder product removal.

On examining our results for E_a for the four cases, we find that both expanding the Rh-Rh distance and replacing substrate metal atoms by MgO contribute to lowering E_a ; both effects are comparable in magnitude, though the latter seems more important. We note that E_a is lowered by 0.42 eV if one considers the effect of strain alone, by 0.94 eV if one considers the effect of changing the chemical nature of the substrate alone, and by 1.65 eV if one considers the effect of both together, i.e., there is some evidence for a synergistic effect. It is interesting to see whether both effects can be encapsulated within a single parameter. One obvious candidate is E_d , the position of the d -band center relative to the Fermi level, which has earlier been posited as a good indicator of the catalytic activity of transition metals.¹⁷ Another quantity, which is related but even simpler to compute, is the “effective coordination number” (described in more detail below), which has been shown to correlate well with surface core level shifts in Rh (Ref. 18) and adsorption energies of NO on Rh.⁵

The effective coordination number serves as a measure of the ambient electronic density (from other, neighboring atoms) that a surface Rh atom is embedded in. It takes into account the local environment of the surface Rh atom by incorporating information about which chemical species the neighbors are, as well as how far away they are. This is done by using the formula

$$n_e = \sum_j \rho_j^{at}(R_j) / \rho_{Rh}^{at}(R_{bulk}), \quad (1)$$

where the sum runs over all neighboring atoms j which are at a distance R_j from the atom under consideration, $\rho_j^{at}(R)$ and $\rho_{Rh}^{at}(R)$ are the atomic charge densities at a distance R away from the nucleus of an isolated atom of the species j or Rh, respectively, and R_{bulk} is the nearest-neighbor distance in bulk Rh. Note that we are approximating the actual density distribution from neighboring atoms by the atomic density; $\rho_{Rh}^{at}(R)$ is evaluated by performing a pseudopotential-based DFT calculation for a single Rh atom. The relevant values of R are near the tail of the atomic charge density where the actual and the pseudosized wave functions match exactly. We point out that evaluating Eq. (1) for a system (where the

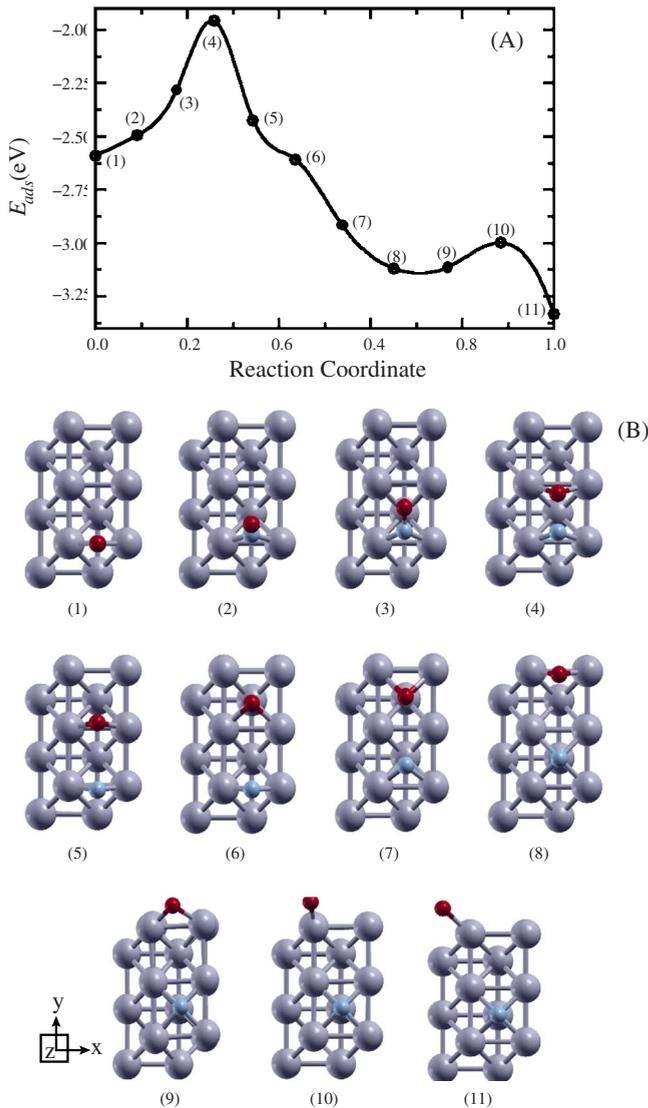


FIG. 3. (Color online) (a) Variation in E_{ads} along the path connecting initial and final states in the dissociation of NO in case (a), and (b) adsorption geometry along the path connecting initial and final states in the dissociation of NO in case (a), where $E_{ads} = E_i - E_{slab} - E_{NO}$, E_{slab} , E_i , and E_{NO} are the total energies of the clean slab, the i th image and the NO molecule in its gas phase, respectively. Gray, blue, and red spheres represent Rh, N, and O atoms, respectively. Note that the N atoms are not visible in the first few images as they lie directly below the O atoms.

atomic arrangement is at least approximately known) is extremely simple since one need not perform additional electronic-structure calculations to obtain the densities on the right-hand side of the equation. We note that a similar parameter plays a crucial role in many popular semiempirical many-body potentials, such as those obtained using the embedded atom method or effective-medium theory.

For bulk Rh, the above formula gives $n_e = 12$, which is the coordination number in the face-centered-cubic structure. As we proceed from system (a) to system (d), n_e gets progressively lowered due to strain and/or the replacement of substrate Rh atoms by Mg and O; it has values of 8.49, 6.65, 5.51, and 3.59, for systems (a), (b), (c), and (d), respectively.

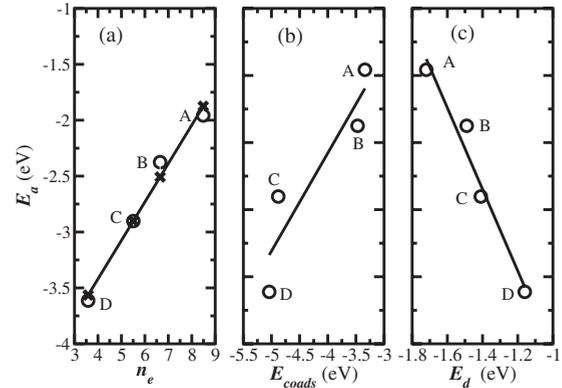


FIG. 4. Variation in the NO activation barrier (E_a) with (a) the effective coordination n_e , (b) the reaction energy E_{coads} , and (c) the position of the d -band center E_d . Note that (b) corresponds to the BEP relationship. The open circles denote the results from our calculations to which we have fitted straight lines using linear regression. The crosses show the predicted value of the activation energy from the linear relationship between E_a and n_e . All energies are referred to the molecule in the gas phase. A, B, C, and D beside the circles are used to relate the data points with the four different systems studied in this Brief Report.

We note that for (a) and (b) the nominal coordination number of the surface Rh atoms is 8 while for (c) and (d) it is 4.

Indicators that correlate with activation energies are extremely useful quantities since the latter can be quite difficult and/or tedious to compute. In addition to the already mentioned d -band center E_d , there is the well-known Bronsted-Evans-Polanyi (BEP) relationship,^{19,20} according to which the coadsorption energy E_{coads} , varies linearly with the activation energy E_a ; it has been shown^{21,22} that this holds true for a wide range of dissociation reactions. We now check how well these two indicators, as well as n_e , work for the cases we have studied here. E_d is obtained using the formula $E_d = \int g_d(\epsilon) \epsilon d\epsilon / \int g_d(\epsilon) d\epsilon$, where $g_d(\epsilon)$ is the d -band projected density of states of the surface Rh atoms, evaluated at energy ϵ . In Fig. 4, we show how the activation energy E_a varies with n_e , the indicator proposed by us, as well as with the well-established indicators E_{coads} and E_d . For all three indicators, the relationship between E_a and the indicator is monotonic and approximately linear. From Fig. 4(a), we see that n_e functions admirably as a predictor of activation energy; $E_a \sim -4.80 + 0.34n_e$, with a correlation coefficient r of 0.99, the mean-squared deviation (MSD) about the regression is 0.01 eV², and the maximum error [that occurs for case (b)] is 0.13 eV. The BEP relation is found to hold reasonably true, with $E_a \sim 0.34 + 0.73E_{coads}$ and $r = 0.92$ [Fig. 4(b)]; the quality of fit is comparable to that found by previous authors,²³ with a maximum error of 0.32 eV [for case (c)] and a MSD of about 0.12 eV². Similarly, for E_d , $E_a \sim -(7.10 + 3.04E_d)$, with $r = -0.98$ [see Fig. 4(c)], with a maximum error of 0.2 eV [for case (b)] and a MSD of 0.03 eV². Note that r serves as a measure of linear association, the closer it is to 1.0, the more perfect the linear relationship. We therefore conclude that n_e performs as well as the other already well-established indicators, as a predictor of dissociation barriers for the model systems considered here. Why

does n_e function as a good indicator of activation energy? While it has generally been acknowledged that lowering coordination number promotes adsorption of reactants and products, the notion of “coordination number” has been somewhat vague and imprecise. Within a tight-binding approach to electronic structure, it is clear that the spread in energies of a band is controlled both by the number of neighbors and the spatial overlap integrals between the wave functions of neighboring atoms. The definition of n_e used in this paper encapsulates both effects, since it involves a sum over (all) atoms in the system as well as the *relative* contribution to overlap integrals, which can be reasonably approximated by seeing how the tail of the atomic density falls off with distance. We note that though the sum is over all atoms, in practice, the major contribution will come from atoms in the immediate vicinity of the atom under consideration. When n_e is lowered, the bandwidth decreases and its center shifts closer to the Fermi energy. This leads to greater overlap between adsorbate and catalyst states, and this in turn (via the BEP relationship) leads to a lower activation energy.

Thus, for the four systems considered by us, we find that the very simple indicator n_e , which is a property of the catalyst alone, and does not even require an electronic-structure calculation in order to be computed (assuming that there is at least a good estimate of the structure of the catalyst), works remarkably well in predicting activation energies. The activation energy changes considerably when going from case (a) to case (d), and it is interesting to find that n_e is able to serve as a predictor of E_a over this wide range in energy, with an error that is small compared to the range of energies under consideration. We have shown that n_e can incorporate the effects of both strain and a change in the chemical nature of the substrate. Other simple ways of changing n_e would be to make the surface rough (e.g., by creating an steps on the surface), or by alloying with another element in the surface

layer; both effects have been shown, by previous authors,^{4,24} to affect barriers, and they will also obviously affect n_e . It remains to be explored to what extent n_e can correctly encapsulate all such changes in the environment of catalyst atoms (one can expect it to fail in some cases, such as when there is significant charge transfer between the catalyst atoms and the substrate, since in such cases the superposition of atomic densities can be expected to be a poor approximation).

We are of course aware that we have only shown that n_e serves as a good indicator for the four cases studied here. However, in this Brief Report, we hope that we have, at the very least, made a case that n_e should be computed for several other systems, so as to establish the parameters within which it functions as a good indicator for activation energies; we hope that our work will stimulate other researchers to compute the values of n_e for the systems and reactions studied by them. If n_e is found to work well also for other systems, then it can serve as a very simple but useful guideline in deciding which systems could be screened as possibly good catalysts, by searching for a system where the activation energy falls within the desired range of the “volcano plot.”

In conclusion, we have studied the dissociation of NO on Rh, and shown that the presence of an MgO substrate contributes to lowering the activation energy, both due to the chemical nature of the substrate and due to the strain imposed by the larger lattice constant of the substrate. Both these effects are well captured by the effective coordination number n_e , which appears to correlate linearly with the activation energy.

We acknowledge support from the Indo-Italian Programme of Cooperation in Science and Technology, administered jointly by the Department of Science and Technology, India, and the Ministry of External Affairs, Italy.

¹B. Hammer and J. K. Nørskov, in *Chemisorption and Reactivity on Supported Clusters and Thin Films*, edited by R. M. Lambert and G. Pacchioni (Kluwer Academic, The Netherlands, 1997), pp. 285–351.

²D. Loffreda, D. Simon, and P. Sautet, *J. Chem. Phys.* **108**, 6447 (1998).

³D. Loffreda, F. Delbecq, D. Simon, and P. Sautet, *J. Chem. Phys.* **115**, 8101 (2001).

⁴D. Loffreda, D. Simon, and P. Sautet, *J. Catal.* **213**, 211 (2003).

⁵R. Pushpa, P. Ghosh, S. Narasimhan, and S. de Gironcoli, *Phys. Rev. B* **79**, 165406 (2009).

⁶P. Giannozzi *et al.*, *J. Phys.: Condens. Matter* **21**, 395502 (2009).

⁷D. Vanderbilt, *Phys. Rev. B* **41**, 7892 (1990).

⁸J. P. Perdew, K. Burke, and M. Ernzerhof, *Phys. Rev. Lett.* **77**, 3865 (1996).

⁹M. Methfessel and A. T. Paxton, *Phys. Rev. B* **40**, 3616 (1989).

¹⁰H. J. Monkhorst and J. D. Pack, *Phys. Rev. B* **13**, 5188 (1976).

¹¹N. W. Ashcroft and N. D. Mermin, *Introduction to Solid State Physics*, 5th ed. (Wiley & Sons, Texas, 1976).

¹²F. Bondino, G. Comelli, A. Baraldi, E. Vesselli, R. Rosei, A. Goldoni, S. Lizzit, C. Bungaro, S. de Gironcoli, and S. Baroni, *J.*

Chem. Phys. **119**, 12525 (2003).

¹³S. Nokbin, J. Limtrakul, and K. Hermansson, *Surf. Sci.* **566-568**, 977 (2004).

¹⁴R. W. G. Wyckoff, *Crystal Structures*, 2nd ed. (Interscience, New York, 1964).

¹⁵B. G. Johnson, P. M. W. Gill, and J. A. Pople, *J. Chem. Phys.* **98**, 5612 (1993).

¹⁶G. Henkelman, B. P. Uberuaga, and H. Jonsson, *J. Chem. Phys.* **113**, 9901 (2000).

¹⁷B. Hammer and J. K. Nørskov, *Surf. Sci.* **343**, 211 (1995).

¹⁸A. Baraldi *et al.*, *New J. Phys.* **9**, 143 (2007).

¹⁹J. N. Bronsted, *Chem. Rev.* **5**, 231 (1928).

²⁰M. G. Evans and N. P. Polanyi, *Trans. Faraday Soc.* **34**, 11 (1938).

²¹T. Bligaard, J. K. Nørskov, S. Dahl, J. Matthiesen, C. H. Christensen, and J. Sehested, *J. Catal.* **224**, 206 (2004).

²²A. Michaelides, Z.-P. Liu, C. J. Zhang, A. Alavi, D. A. King, and P. Hu, *J. Am. Chem. Soc.* **125**, 3704 (2003).

²³T. R. Munter *et al.*, *Phys. Chem. Chem. Phys.* **10**, 5202 (2008).

²⁴C. J. Zhang, R. J. Baxter, P. Hu, A. Alavi, and M. H. Lee, *J. Chem. Phys.* **115**, 5272 (2001).